

**SYNTHESIS OF CARBON NANOTUBES VIA
DECOMPOSITION OF METHANE USING CARBON
SUPPORTED CATALYSTS**

by

SIVAKUMAR VAIYAZHIPALAYAM MURUGAIYAN

**Thesis submitted in fulfilment of the requirements
for the degree of
Doctor of Philosophy**

May 2011

*This Thesis is dedicated to my beloved Father
Late. Mr. V. M. Murugaiyan and
all my family members*

ACKNOWLEDGEMENT

My foremost sincere appreciation is forwarded to my main supervisor, Prof. Dr. Abdul Rahman Mohamed, for granting me the opportunity to pursue my PhD in Chemical Engineering at Universiti Sains Malaysia (USM), Malaysia. I place on record my indebtedness to him for being an excellent advisor, taking precious time of his busy schedule to supervise my research activities and giving me expert guidance, constant attention, valuable comments and enthusiastic support throughout the whole course of my research study.

My heartfelt thanks also go to my co-supervisor, Assoc. Prof. Dr. Ahmad Zuhairi Abdullah, for providing constructive criticisms, fruitful discussions, incessant support, guidance and encouragement during my studies. I would also like to thank Prof. Dr. Azlina Harun Kamaruddin, Dean of the School of Chemical Engineering USM, Assoc. Prof. Dr. Lee Keat Teong and Assoc. Prof. Dr. Mohamad Zailani Abu Bakar, Deputy Deans of the School of Chemical Engineering, for their continuous motivation, and invaluable help in postgraduate affairs throughout my studies. I would also like to extend my sincere appreciation to all professors and lecturers in this school especially to Prof. Subhash Bhatia, Assoc. Prof. Dr. James Noel Fernando, Dr. Siang Piao Chai, Dr. Vel Murugan and Dr. Zainal Ahmad, who have shared their precious knowledge and experience with me. I extend my gratitude to all the laboratory technicians and administrative staffs of the School of Chemical Engineering USM, for the assistance rendered.

I would also like to take the opportunity to thank all of my friends at USM, for making my stay at the university very cherishable and memorable. I would like to

express my genuine gratitude to my dearest mother (Mrs. Santhamani), my loving wife (Anitha), my daughter (Thitiksha), my sister (Sivagami), my brother-in-law (Mr. Balaji) and all my in-laws for their great patience, love, moral support and utmost care. They are always on my side, riding along with me on my ups and downs as well as giving me encouragement to pursue my dreams. His enduring sacrifice to enable me to have a better future will be remembered forever. My deepest thanks to all the members of Ganeson thatha family for their hospitality in Malaysia.

It is with high esteem I wish to express my sincere thanks to the Ministry of Science, Technology and Innovation (MOSTI), Malaysia and Universiti Sains Malaysia for offering me support through their research project (Project No: 03-01-05-SF0125) and Research Fellowship during my candidature period. Also, I would like to express my sincere thanks to the Correspondent, Secretary, Principal, Administrative Officer, Head of Chemical Engineering Department and my colleagues at Coimbatore Institute of Technology (CIT), Coimbatore, India for providing me an opportunity to pursue my PhD in Chemical Engineering at USM, Malaysia by granting study leave.

SIVAKUMAR VAIYAZHIPALAYAM MURUGAIYAN

MAY, 2011

TABLE OF CONTENTS

	Page
ACKNOWLEDGEMENT	ii
TABLE OF CONTENTS	iv
LIST OF TABLES	ix
LIST OF FIGURES	xi
LIST OF PLATES	xvii
LIST OF ABBREVIATIONS	xviii
LIST OF SYMBOLS	xxi
ABSTRAK	xxiv
ABSTRACT	xxvi
CHAPTER 1 INTRODUCTION	
1.1 Nanoscience and nanotechnology	1
1.2 Future scope of nanotechnology	2
1.3 Carbon and its classification	4
1.4 Carbon nanotubes (CNTs) morphologies and its properties	6
1.5 Applications of CNTs	11
1.6 Problem statement	13
1.7 Research objectives	16
1.8 Scope of the study	17
1.9 Organization of thesis	19
CHAPTER 2 LITERATURE REVIEW	
2.1 CNT synthesis methods	21
2.1.1 Arc- discharge method	21
2.1.2 Laser ablation method	23
2.1.3 Chemical vapour deposition (CVD) method	24
2.1.4 Summary	25
2.2 Modified chemical vapour deposition methods	26
2.3 Nature of hydrocarbon sources in CVD process	30
2.3.1 Various hydrocarbon sources	30
2.3.2 Methane chemical vapour deposition (m-CVD) method	36

2.4	CNTs growth parameters	45
2.4.1	Catalysts	45
2.4.2	Metal catalyst – support interaction in CNTs synthesis	49
2.4.3	Metal as catalyst promoters in CVD reactions	52
2.5	Carbon as catalyst support	54
2.5.1	Role of carbon in methane decomposition	55
2.5.2	Carbon as support in CNTs synthesis	61
2.6	CVD reaction parameters influence in CNTs synthesis	64
2.7	Growth mechanisms of CNTs	68
2.8	Kinetic studies in methane CVD process	71
CHAPTER 3 MATERIALS AND METHODS		74
3.1	Materials and chemicals	74
3.2	Experimental rig setup	75
3.2.1	Gas mixing section	75
3.2.2	Reaction section	79
3.2.3	Gas analysis section	80
3.3	Overall experimental flowchart	81
3.4	Screening of carbon supports	82
3.5	Screening of active metal components	83
3.5.1	Catalyst preparation	84
3.5.2	Methane decomposition and CNTs synthesis study	86
3.5.3	Blank study	87
3.5.4	Process parameter analysis and optimization	88
3.6	Kinetic study	90
3.7	Catalysts and CNTs characterization studies	91
3.7.1	Surface characteristics	91
3.7.2	Temperature programmed reduction (TPR)	91
3.7.3	Scanning electron microscopy (SEM)	92
3.7.4	Transmission electron microscopy (TEM)	92
3.7.5	Thermal gravimetric analysis (TGA)	93
3.7.6	X-ray Diffraction technique (XRD)	93
3.7.7	Raman spectroscopy	94

CHAPTER 4 RESULTS AND DISCUSSIONS	95
4.1 Study of carbon support materials properties	96
4.1.1 Thermal stability studies of the raw carbon supports	98
4.1.2 XRD Characterization of raw carbon supports	99
4.1.3 Raman characterization of raw carbon supports	102
4.1.4 Blank study of the carbon supports in methane decomposition and CNTs synthesis	103
4.1.5 Study of carbon molecular sieve supported catalysts	105
4.1.6 Study of activated carbon supported catalysts	111
4.1.7 Summary of the preliminary study of carbon supports	118
4.2 Methane decomposition studies over Ni/AC catalyst	119
4.2.1 Effect of Ni loading in AC support	119
4.2.2 Effect of Ni/AC reduction temperature	122
4.2.3 Effect of methane CVD reaction temperature on Ni/AC catalyst	124
4.2.4 TEM characterization	128
4.2.5 Thermal stability of CNTs synthesized using Ni/AC catalyst	132
4.2.6 Effect of reaction time	135
4.2.7 XRD characterization	136
4.2.8 Raman spectrum characterization study	138
4.2.9 Summary of Ni/AC catalyst performance in m-CVD process and CNTs synthesis	139
4.3 Methane decomposition studies using AC-supported Co catalyst	142
4.3.1 Effect of Co metal loading	142
4.3.2 Effect of Co/AC catalyst calcination and its reduction profile	143
4.3.3 Effect of methane CVD reaction temperature on Co/AC catalyst	145
4.3.4 Effect of catalyst reduction temperatures during m-CVD reaction	147
4.3.5 TEM characterization	148
4.3.6 Thermal stability of CNTs developed on Co/AC catalyst	151

4.3.7	XRD characterization	153
4.3.8	Summary of Co/AC catalyst behaviors in CNTs formation	154
4.4	Methane decomposition studies using AC-supported Fe catalyst	155
4.4.1	Effect of Fe metal loading	155
4.4.2	Effect of reduction temperature on Fe /AC catalyst	157
4.4.3	Effect of m-CVD reaction temperature	158
4.4.4	XRD characterization studies	160
4.4.5	TEM characterization studies	162
4.4.6	Thermogravimetric analysis	164
4.4.7	Raman spectra characterization study	168
4.4.8	Summary of m-CVD process and CNTs synthesis over Fe/AC catalyst	169
4.5	Comparative studies of AC-supported active metal catalyst	169
4.5.1	Methane conversion and H ₂ production	170
4.5.2	As-synthesized CNTs samples surface morphology analysis	171
4.5.3	Thermogravimetric analysis	174
4.5.4	Raman Spectra results	176
4.6	Process optimization studies using DoE	178
4.6.1	Process variables and the response	178
4.6.2	Model selection and ANOVA	179
4.6.3	Response studies using surfafce plots	182
4.6.4	Optimization studies	185
4.7	Growth mechanism and Kinetic studies	187
4.7.1	Order of m-CVD reaction	191
4.7.2	Activation energy determination	193
4.7.3	Kinetic studies	195
CHAPTER 5 CONCLUSIONS AND RECOMMENDATIONS		201
5.1	Conclusions	201
5.2	Recommendations	204
REFERENCES		206

APPENDICES	226
Appendix A FTIR Data	226
Appendix B Gas Chromatograph Results	227
Appendix C Sample Calculations	229
LIST OF PUBLICATIONS	233

LIST OF TABLES

		Page
Table 1.1	Properties of carbon Nanotubes (Dong <i>et al.</i> , 2007)	10
Table 1.2	Different fields of applications of carbon nanotubes	12
Table 2.1	Summary and comparison of CNTs synthesis methods (Baddour and Briens, 2005)	26
Table 2.2	Summary of the CVD reactions during CNTs synthesis with various hydrocarbon sources with other inert gas mixtures	32
Table 2.3	Summary of the literatures with methane as hydrocarbon source in CVD reaction for CNTs synthesis	38
Table 2.4	Recent studies on using carbon as catalyst in thermal methane decomposition reactions	58
Table 3.1	List of chemicals and reagents	74
Table 3.2	Major components of the experimental rig and their functions	76
Table 3.3	Gas chromatograph retention time of each detected gas component	80
Table 3.4	Synthesized catalysts over different types of carbon supports and their labeling	85
Table 3.5	Experimental conditions considered in this study	87
Table 3.6	Experimental conditions for methane decomposition based on factorial design using RSM	90
Table 4.1	Proximate analysis results of support carbon materials	96
Table 4.2	Ultimate analysis of support carbon materials	97
Table 4.3	Surface characteristics of activated carbon materials	97
Table 4.4	Methane conversion results obtained over raw carbon support materials subjected to three different m-CVD temperatures (650, 750 and 850 °C) reported maximum at 10 th min of CVD	103

Table 4.5	Methane conversion over 5 wt% (Co, Fe and Ni / CMS-G) catalysts at different m-CVD temperatures (650, 750 and 850 °C) reported under gas flow (CH ₄ :N ₂ = 1:2) ratio	107
Table 4.6	Effect of Co metal loadings and reaction temperatures on CH ₄ conversions at CVD time of 10 min.	145
Table 4.7	Comparison of CH ₄ conversion for AC supported Ni, Co and Fe catalysts at a specified m-CVD process conditions	170
Table 4.8	Comparison of the morphologies of CNTs formed over different types of catalyst	173
Table 4.9	Summary of carbon amounts over Ni/AC, Co/AC and Fe/AC catalysts and their respective thermal oxidation temperatures	175
Table 4.10	Experimental matrix of the three-level factorial design of response surface methodology (RSM) for 5 wt% Fe/AC catalyst for CH ₄ :N ₂ ratio of 1:2	179
Table 4.11	Sequential model sum of squares for Fe/AC catalyst	180
Table 4.12	ANOVA table for methane conversion according to the quadratic model	181
Table 4.13	The preset goals with the constraints for all the independent factors and response in the numerical optimization	186
Table 4.14	Reproducibility test under optimum condition over Fe/AC catalyst	186
Table 4.15	Values of reaction rate constants (k) at various reaction temperatures	194

LIST OF FIGURES

		Page
Figure 1.1	Scale showing the range of materials from mm to nm (Serrano <i>et al.</i> , 2009)	1
Figure 1.2	Diverse applications of nanotechnology in today's life (Bioinfobank, 2010)	2
Figure 1.3	Nanotechnology related area of services and future estimation by National Science Foundation (NSF), USA (Interdisciplines, 2010)	4
Figure 1.4	Classification of carbon based on its nature (Baddour and Briens, 2005)	5
Figure 1.5	Allotropes of carbon and their structural arrangement (Nanoage, 2010)	6
Figure 1.6	Structures of (a) Unique CNT, (b) Single-walled and (c) Multi-walled carbon nanotubes (Danmengshuai, 2010)	7
Figure 1.7	Chirality and related structure of CNTs (Wildoer <i>et al.</i> , 1998)	8
Figure 2.1	Schematic diagram of the Arc-discharge method of CNTs synthesis (Ando <i>et al.</i> , 2004)	22
Figure 2.2	Schematic diagram of the Laser ablation method of CNTs synthesis (van der Wal <i>et al.</i> , 2003)	23
Figure 2.3	Schematic diagram of a CVD process for CNTs synthesis (Oncel and Yurum, 2006)	24
Figure 2.4	Classification of CVD process according to their energy sources	30
Figure 2.5	Support surface showing the three different types of pore structure (Rodriguez-Reinoso, 1998)	54
Figure 2.6	Network of the important factors for CNTs synthesis	67
Figure 2.7	Schematics of the growth mechanism: (a) Base growth and (b) tip growth models (Lee <i>et al.</i> , 2000)	70
Figure 3.1	Schematic diagram of the experimental rig setup	77
Figure 3.2	Schematic diagram of horizontal fixed-bed reactor system.	79

Figure 3.3	Flowchart of overall experimental activities involved in this study	81
Figure 3.4	Metals selected for catalyst development in this study	83
Figure 4.1	Thermogravimetric analysis curves of different types of raw carbon support material (a) AC, (b) CMS- IN and (c) CMS-G	99
Figure 4.2	XRD patterns of raw carbon support materials (a)AC (b) CMS-IN and (c) CMS-G	101
Figure 4.3	Raman spectra of three different raw carbon supports	102
Figure 4.4	TEM images of products of (a) CMS-IN and (b) CMS-G and (c) AC after blank study conducted at an m-CVD temperature of 850 °C	105
Figure 4.5	SEM image showing the surface topography of 5 wt% Co/CMS-G catalyst	106
Figure 4.6	TEM images of products obtained over (a) Co/CMS-G (b) Fe/CMS (c) Ni/CMS-G catalysts at m-CVD temperature 750 °C (d) Co/CMS-G (e) Fe/CMS-G (f) Ni/CMS-G catalyst at m-CVD of 850 °C	109
Figure 4.7	Model diagram showing the carbon molecular sieve (CMS) supports and metal catalyst particles distribution during m-CVD process	111
Figure 4.8	Methane conversion versus time for three different catalysts at m-CVD temperature of 750 °C	112
Figure 4.9	TEM images of product samples obtained using 5 wt% metal loading (a) Ni/AC (b) Fe/AC and (c) Co/AC catalysts	114
Figure 4.10	SEM images showing the surface topography of the 5 wt% (a) Fe/AC (b) Co/AC and (c) Ni/AC catalyst (before m-CVD)	115
Figure 4.11	Model diagram showing the activated carbon (AC) support and metal particles distribution during m-CVD process	117
Figure 4.12	Effect of Ni metal loading over AC support subjected to calcination(C) of 450 °C in CH ₄ conversion at different reduction(r) and CVD reaction(R) temperatures	121
Figure 4.13	Effect of Ni/AC catalyst reduction temperature on CH ₄ conversion at reaction temperature of 750 °C, at different catalyst calcination and reduction temperatures	123

Figure 4.14	Effect of m-CVD reaction (R) temperature and gas flow ratio in CH ₄ conversion at calcination (C = 350 °C) and reduction (r = 550 °C) on 5 wt% Ni/AC catalyst [*gas ratio (CH ₄ : N ₂ = 1:3)]	124
Figure 4.15	TPR profile of Ni/AC catalyst subjected to different calcination temperatures of (a) 350 °C and (b) 450 °C	126
Figure 4.16	TPR profile of raw AC catalyst subjected to different calcination temperatures of 350 °C (AC - C1) and 450 °C (AC - C2)	127
Figure 4.17	TEM images of as-synthesized product obtained using 5 wt% Ni/AC catalysts under different experimental conditions (a) calcined (350 °C) reduced (450 °C) Reaction (650 °C); (b) calcined (450 °C) reduced (550 °C) Reaction (850 °C); (c) calcined (350 °C) reduced (550 °C) Reaction (850 °C) and (d) calcined (450 °C) unreduced Reaction (750 °C)	129
Figure 4.18	TEM images of the product samples after m-CVD reaction at 850 °C (a) for CH ₄ : N ₂ = 1: 3 gas flow ratio; (b) for reaction time of 90 min	131
Figure 4.19	TGA plot of product samples subjected to varying calcination, reduction conditions and at reaction temperatures of 750 °C	133
Figure 4.20	TGA plot of product samples subjected to varying calcination, reduction conditions and at reaction temperatures of 850 °C	134
Figure 4.21	DTA plot of synthesized CNTs sample subjected to reduction at 550 °C with varying calcinations (cal = 350 & 450 °C) and reaction temperatures (R= 750 & 850 °C)	135
Figure 4.22	TEM images showing MWNTs obtained over Ni/AC catalyst after m-CVD reaction time of (a) 60 min and (b) 90 min	136
Figure 4.23	XRD plot of the 5 wt% Ni/AC sample after calcined (350 °C) and reduced with H ₂ at 550 °C; (a) before m-CVD and (b) after m-CVD at 850 °C	137
Figure 4.24	Raman spectrum data for AC support and Ni/AC catalyst before and after m-CVD reaction	138
Figure 4.25	Effect of Ni- metal loadings upon methane conversion values at 10 th min reaction time of with Ni/AC catalyst	141
Figure 4.26	Effect of m-CVD reaction temperatures on methane conversions at 10 th min of reaction time with 5 wt% Ni/AC	141

	catalyst	
Figure 4.27	Effect of Co loadings on CH ₄ conversions for catalyst calcined at 350 °C, reduced at 450 °C and reaction at temperature at 750 °C	143
Figure 4.28	TPR profiles of 5 wt% Co/AC catalyst subjected to two different calcination temperatures (a) 5 Co-C1 at 350 °C and (b) 5 Co-C2 at 450 °C	144
Figure 4.29	Influence of reduction temperature on 15 wt% Co/AC catalysts (a) calcined at 350 °C, unreduced; (b) calcined, reduced at 350 °C; (c) calcined at 350 °C, reduced at 450 °C; (d) calcined at 350 °C, reduced at 550 °C in methane conversion at CVD temperature of 850 °C	148
Figure 4.30	TEM images of carbon deposits on 15 wt% Co/AC catalyst, calcined (350 °C); reaction (850 °C) (a) unreduced; (b) reduction (350 °C); (c) reduction (350 °C) and reaction (750 °C); (d) reduction (450 °C) and reaction (850 °C); (e) reduction (550 °C) and reaction (850 °C)	150
Figure 4.31	TGA profile of product samples obtained with 15 wt% Co/AC catalyst calcined at 350 °C showing (a) unreduced; (b) reduced at 450 °C and (c) reduced at 550 °C under m-CVD reaction temperature of 850 °C conditions	151
Figure 4.32	DTA plot of product samples from 15 wt% Co/AC catalyst subjected to varying experimental conditions (a) calcined at 350 °C, reduced at 450 °C; un-reacted (b) calcined at 350 °C, reduced at 450 °C, CVD at 850 °C; (c) calcined at 350 °C, reduced at 550 °C, CVD at 850 °C	152
Figure 4.33	XRD patterns for the Co/AC catalyst with different pre-treatment conditions (a) only calcined at 350 °C (b) calcined followed by reduction at 450 °C and (c) calcined, reduced, after m-CVD reaction at 850 °C	153
Figure 4.34	Plot showing the effect of Co-metal loading upon methane conversion under best optimized conditions of calcination (350 °C) and reduction (450 °C) for the Co/AC catalyst	154
Figure 4.35	Effect of Fe metal loading on CH ₄ conversion as a function of time for catalyst samples calcined at 350 °C, reduced under H ₂ at 450 °C and CVD temperature at 750 °C	156
Figure 4.36	Temperature programmed reduction (TPR) profiles of raw AC support with 5 wt % of Fe loading: (a) calcined at 350 °C, (b) calcined at 450 °C	157
Figure 4.37	Profiles of CH ₄ conversion as a function of time for 5 wt % Fe/AC catalysts at the reaction temperature of 750 °C: (a)	159

	calcined at 350 °C; (b) calcined at 350 °C and reduced at 450 °C; (c) calcined at 350 °C and reduced at 550 °C	
Figure 4.38	Profiles of CH ₄ conversion as a function of time for 5 wt% Fe/AC catalysts at the reaction temperature of 850 °C: (a) calcined at 350 °C; (b) calcined at 350 °C and reduced at 450 °C; (c) calcined at 350 °C and reduced at 550 °C	160
Figure 4.39	XRD patterns of Fe/AC catalyst calcined at 350 °C: (a) raw AC support; (b) unreduced; (c) reduced at 450 °C; (d) reduced at 550 °C; Fe ₂ O ₃ (Δ); Fe ₃ O ₄ (○); FeO (◆)	161
Figure 4.40	TEM images of as-synthesized CNTs from 5 wt% Fe/AC catalyst calcined at 350 °C, CVD at 850 °C: (a) unreduced (1 - MWNT, 2 - tip-growth mechanism, 3 - encapsulated catalyst; (b) reduced at 450 °C (4 - broad nano filamentous carbons); (c) reduced at 450 °C, reaction at 750 °C	163
Figure 4.41	TGA plot of as-synthesized samples formed over 5 wt % Fe/AC catalyst at CVD temperature of 750 °C: (a) unreduced; (b) reduced at 450 °C; (c) reduced at 550 °C	164
Figure 4.42	DTA plot of as-synthesized samples formed over 5 wt % Fe/AC catalyst at CVD temperature of 750 °C: (a) unreduced; (b) reduced at 450 °C; (c) reduced at 550 °C	165
Figure 4.43	TGA plots of as-produced samples from 5 wt % Fe/AC catalyst used at CVD temperature of 850 °C: (a) unreduced; (b) reduced at 450 °C; (c) reduced at 550 °C	166
Figure 4.44	DTA plot of as-produced samples from 5 wt % Fe/AC catalyst at CVD temperature of 850 °C: (a) unreduced; (b) reduced at 450 °C; (c) reduced at 550 °C	167
Figure 4.45	Raman spectrum for AC support and Fe/AC catalyst, before and after the m-CVD reaction	168
Figure 4.46	Plot of half-life time of three different metal catalysts during m-CVD based on its activity in CH ₄ conversion under respective best conditions	171
Figure 4.47	SEM/EDX analysis result of the product samples showing CNTs morphologies that grown on (a) Ni/AC, (b) Co/AC and (c) Fe/AC catalyst	172
Figure 4.48	TEM images of thin-walled CNTs formed at 750 °C over Ni/AC catalyst (a) with measured dimension, (b) without catalyst at its tip	174
Figure 4.49	TG plot of synthesized un-reacted Ni, Co and Fe/AC supported catalysts	176

Figure 4.50	Raman spectra of product samples obtained using Ni/AC, Co/AC and Fe/AC catalysts under their optimized m-CVD conditions of higher CH ₄ conversion	177
Figure 4.51	Parity plot of actual and predicted values of methane conversion	182
Figure 4.52	Response surface plot for the effect of Fe loading and catalyst reduction temperature on methane conversion	184
Figure 4.53	Response surface plot for the effect of Fe loading and m-CVD reaction temperature on methane conversion	184
Figure 4.54	Response surface plot for the effect of Fe/AC catalyst reduction and m-CVD reaction temperature on methane conversion	185
Figure 4.55	HRTEM image of tip-growth MWNT over Fe/AC catalyst with Fe-metal particle embedded within the CNTs	189
Figure 4.56	Proposed CNTs growth model with sequence of steps via m-CVD process over Fe/AC catalysts	190
Figure 4.57	Log plot of methane partial pressure and initial reaction rate for m-CVD over 5 wt% Fe/AC catalyst at different temperatures	192
Figure 4.58	Arrhenius plot of rate constant (ln k) and reaction temperature (1/T) over Fe/AC catalyst	195
Figure 4.59	Plot of m-CVD reaction initial rate and partial pressures upon 5 wt% Fe/AC catalyst at different reaction temperatures	199

LIST OF PLATES

	Page
Plate 3.1 Experimental rig setup and other major components	78

LIST OF ABBREVIATIONS

AC	Activated carbon
ACCVD	Alcohol catalytic chemical vapour deposition
AFM	Atomic force microscope
ANOVA	Analysis of variance
BEI	Back scattering electron imaging
BET	Brunauer Emmet Teller method
CB	Carbon black
CCVD	Catalytic chemical vapour deposition
CFC	Carbon fibre composites
CMS	Carbon molecular sieves
CMS-G	Carbon molecular sieves-Germany
CMS-IN	Carbon molecular sieves-India
CNFs	Carbon nanofibres
CNTs	Carbon nanotubes
CNWs	Carbon nanowires
CRTs	Cathode ray tubes
CVD	Chemical vapour deposition
DCPECVD	Direct current plasma enhanced chemical vapour deposition
DI	De-ionized
DoE	Design of Experiment
DWNTs	Double walled carbon nanotubes
EDX	Energy dispersive x-ray
FBR	Fluidized bed reactor
FT-IR	Fourier transformed infra-red spectroscope
GC	Gas chromatograph

GE	General electricals
HCNTs	Helical carbon nanotubes
HF	Hot filament
HiPCO	High pressure carbon monoxide
HRTEM	High resolution transmission electron microscope
IBM	International business machine
ICP-CVD	Inductively coupled plasma-chemical vapour deposition
LPTCD	Low pressure thermal catalytic deposition
MCVD	Microwave chemical vapour deposition
MIT	Massachusetts institute of technology
MSI	Metal support interaction
MWNTs	Multi-walled carbon nanotubes
m-CVD	Methane chemical vapour deposition
NSF	National science foundation
PFR	Plug flow reactor
RBM	Radial breathing mode
RDS	Rate determining step
RFCVD	Radio frequency chemical vapour deposition
RSM	Response surface methodology
SEI	Secondary electron imaging
SEM	Scanning electron microscope
SMR	Steam methane reforming
SWNTs	Single-wall carbon nanotubes
TCD	Thermal conductivity detector
TEM	Transmission electron microscope
TGA	Thermogravimetric analysis
TPR	Temperature programmed reduction

VGCF	Vapour grown carbon fibres
XRD	X-ray diffractometer
Y-CNTs	Y-shaped carbon nanotubes

LIST OF SYMBOLS

1-D, 2-D, 3-D	Dimensional structure of carbon
Å	Angstrom
Amp	Amperes
cm ³	Cubic centimeter
C ₆₀	Fullerenes
°C	Degree Centigrade
Cal	Calcination temperature
d	Distance between atomic layers in crystal
dc	Direct Current
D _{crystallite}	Average size of metal crystal
E _a	Activation energy
g	gram
GA	Giga Amperes
Gpa	Giga Pascal
GHz	Giga Hertz
h	hour
i.d.	Internal diameter of CNTs
I _D	Intensity of Defective carbon peaks
I _G	Intensity of Graphitized carbon peaks
J	Joules
k	Kilo
k ₀	Frequency factor
$k_{+1}, k_{+2}, k_{+3}, k_{+4},$ k_{+5}, k_{+6}	Rate constant of forward reaction
$k_{-1}, k_{-2}, k_{-3}, k_{-4},$ k_{-5}, k_{-6}	Rate constant of reverse reaction

$K_1, K_2, K_3, K_4, K_5, K_6$	Ratio of rate constants
K	Kelvin
kJ	Kilo Joules
kPa	Kilopascal
kV	Kilovolts
m^2	Square meter
mA	Milli Amperes
ml	Milli litres
min	minutes
mol	Moles
mm	millimeter
mmol	Millimoles
M_{CH_4}	Molar flow rate of methane (mol/min)
n	Order of reaction
n,m	Integers indicating chiral vectors
nm	nanometer
psi	Pressure per square inches
P_{CH_4}	Partial pressure of methane
r	Reduction temperature
r_{CH_4}	Rate of methane decomposition
r_0	Initial rate of reaction
$r(t)$	Rate of reaction at time (t)
R	Reaction temperature
s, p, sp, sp^2	Electron orbitals
sccm	Standard cubic centimeter per minute
S	Active site on catalyst surface
T	Absolute temperature

TPa	Tetra pascal
vol	Volume
V	Volt
w.t.	Wall thickness of CNTs
wt%	Weight percent

GREEK SYMBOLS

μm	micrometer
λ	Lamda (X-ray wavelength)
β_d	Distance between atomic layers
β_{obs}	Observed line width
β_{inst}	Instrumental line width
θ	Diffraction angle
ω_{RBM}	Raman shift
$\theta_{\text{CH}_3\text{S}}$	Concentration of sites occupied by CH ₃ S
$\theta_{\text{CH}_2\text{S}}$	Concentration of sites occupied by CH ₂ S
θ_{HS}	Concentration of sites occupied by HS
θ_{V}	Concentration of vacant sites
θ_{T}	Concentration of total sites

SINTESIS NANOTUB KARBON MELALUI PENGURAIAN METANA MENGGUNAKAN MANGKIN BERSOKONGKAN KARBON

ABSTRAK

Nanotub karbon dengan sifat khususnya adalah bahan yang menarik dan ditemui aplikasinya dalam pelbagai bidang. Disebabkan kepada permintaan global, sintesisnya pada kos yang lebih rendah tidak dapat dielakkan. Dalam kajian ini, bahan karbon berharga murah seperti penapis molekul karbon (CMS-G, CMS-IN) dan karbon teraktif (AC) dikaji sebagai penyokong kepada tiga jenis logam aktif yang berbeza (Ni, Co dan Fe) untuk proses uraian wap kimia metana (m-CVD) bagi menghasilkan CNTs. Kajian bebas dan aktiviti mangkin diimpregnasikan logam aktif (5, 10 dan 15 wt%) telah dikaji pada suhu 650, 750 dan 850 °C untuk penukaran metana (CH₄) yang maksimum dan pertumbuhan CNTs yang optimum. Mangkin logam yang disintesiskan atas penyokong AC dengan sifat yang diperlukan adalah lebih baik dalam penukaran metana dan pembentukan CNTs berbanding dengan penyokong jenis CMS. Analisis mendalam telah dijalankan keatas mangkin individu seperti Ni/AC, Co/AC dan Fe/AC dengan mempelbagaikan parameter dalam penyediaan mangkin dan keadaan tindak balas. Mangkin 5 wt% Ni/AC dikalsinkan pada 350 °C, terturun pada 550 °C ditemui memberikan penukaran metana yang maksimum sebanyak 96.81% pada suhu 850 °C. Bilangan CNTs yang lebih banyak dengan diameter dalaman purata sebanyak 14 nm dan ketebalan sebanyak 3 nm telah diperoleh melalui keadaan ini. Analisis SEM/EDX telah digunakan untuk memastikan pembentukan CNTs dan kandungan logam atas mangkin yang disintesiskan. Aktiviti mangkin dengan nisbah gas metana kepada nitrogen (CH₄:N₂)

sebanyak 1:2 ditemui dapat diperpanjang dengan lebih baik berbanding nisbah sebanyak 1:3. Profil penurunan berprogramkan suhu (TPR) bagi mangkin Ni/AC menunjukkan bahawa oksida nikel NiO terbentuk di bawah 450 °C. Kajian TEM sampel produk menunjukkan bahawa nanotub karbon berbilang dinding (MWNTs) dengan jenis nipis dan lebih luas berserabut mempunyai diameter dalaman sekitar 2.5 dan 27 nm, masing-masing telah terbentuk dengan 5 wt% Ni/AC di bawah penyediaan dan keadaan tindak balas yang berbeza. Begitu juga, mangkin dengan kemasukan 15 wt% Co/AC, dikalsinkan pada 350 °C dan terturun pada 450 °C merekodkan penukaran metana yang maksimum sebanyak 89% pada 850 °C. MWNTs seperti reben yang berputar dengan diameter dalaman purata sekitar 16 nm telah terbentuk. Mangkin dengan kemasukan 5 wt% Fe/AC melaporkan penukaran metana yang maksimum sebanyak 98.6% pada 750 °C. Aktiviti mangkin diperpanjang lebih daripada 2 h telah ditunjukkan oleh mangkin 5 wt% Fe/AC berbanding dengan mangkin yang lain. Analisis permeteran gravity haba (TGA) menunjukkan bahawa suhu penurunan haba akhir bagi mangkin yang disintesis dan sampel produk adalah dalam urutan Co/AC > Ni/AC > Fe/AC. Nisbah kecacatan karbon grafitik ($I_D : I_G$) yang diperolehi oleh Raman spektrum adalah 1.17, 1.20 dan 1.32 bagi sampel produk dengan mangkin Fe/AC, Ni/AC dan Co/AC, masing-masing. Bagi mangkin yang terbaik (5 wt% Fe/AC), keadaan optimum ditentukan menggunakan permukaan sambutan (RSM) dan analisis variasi (ANOVA) telah dicapai pada penurunan 447 °C, tindak balas pada 806 °C di bawah aliran CH₄:N₂ ratio sebanyak 1:2 dengan 87.25% penukaran CH₄. Mekanisme pertumbuhan MWNTs telah dicadangkan dengan urutan langkah tindak balas. Tenaga pengaktifan dijangkakan sekitar 42.25 kJ/mol. Kadar tindak balas, urutan tindak balas dan kinetiknya telah dikaji dan korelasinya telah disahkan dengan data ujikaji.

SYNTHESIS OF CARBON NANOTUBES VIA DECOMPOSITION OF METHANE USING CARBON SUPPORTED CATALYSTS

ABSTRACT

Carbon nanotubes (CNTs) with their special properties find applications in many areas. Owing to its global demand, its synthesis at a cheaper cost is inevitable. In this study, low-cost carbon materials like carbon molecular sieves (CMS-G, CMS-IN) and activated carbon (AC) were examined as supports for three different active metals (Ni, Co and Fe) for methane chemical vapour decomposition (m-CVD) process to produce CNTs. Blank studies and active metal impregnated (5, 10 and 15 wt% loadings) catalysts activity were studied at temperatures 650, 750 and 850 °C for maximum methane (CH₄) conversion and optimum CNTs growth. The synthesized metal catalysts over AC support were relatively better in CH₄ conversion and formed CNTs compared to CMS type supports. In-depth analysis of individual catalysts like Ni/AC, Co/AC and Fe/AC were made by varying the parameters of catalyst preparation and reaction conditions. 5 wt% Ni/AC catalysts calcined at 350 °C, reduced at 550 °C was found to give maximum CH₄ conversion of 96.81% at 850 °C. Higher population of CNTs with average internal diameter of 14 nm and thickness of 3 nm was obtained under these conditions. SEM/EDX analyses were used to confirm the formed CNTs and metal content on synthesized catalysts. Methane to nitrogen (CH₄:N₂) gas ratio of 1:2 was found to possess prolonged catalyst activity better than a ratio of 1:3. Temperature programmed reduction profiles (TPR) of Ni/AC catalyst showed that nickel oxides NiO formed below 450 °C. TEM study of product samples revealed that multi-walled carbon nanotubes (MWNTs) with thin and broader filamentous type having average internal diameters of around 2.5 and 27 nm, respectively were formed over 5 wt% Ni/AC catalyst under different

preparation and reaction conditions. Similarly, Co/AC catalyst with 15 wt% loading, calcined at 350 °C and reduced at 450 °C recorded a maximum CH₄ conversion of 89% at 850 °C. Twisted *ribbon-like* MWNTs with average internal diameter of around 16 nm were formed. Fe/AC catalysts with 5 wt % loading reported maximum CH₄ conversion of 98.6% at 750 °C. Prolonged catalyst activity of longer than 2 h was demonstrated by 5 wt% Fe/AC catalyst compared to the other catalysts. Thermogravimetric analysis (TGA) showed that the final thermal degradation temperatures of the synthesized catalyst and product samples were in the order of Co/AC > Ni/AC > Fe/AC. Ratios of defective to graphitic carbons (I_D/I_G) that were obtained by Raman spectra were 1.17, 1.20 and 1.32 for product samples obtained with Fe/AC, Ni/AC and Co/AC catalysts, respectively. For the best catalyst (5wt% Fe/AC), optimized condition determined using response surface methodology (RSM) and analysis of variance (ANOVA) studies were achieved at reduction of 447 °C, reaction at 806 °C under flow CH₄:N₂ ratio of 1:2 with 87.25 % CH₄ conversion. MWNTs growth mechanism was proposed with sequence of reaction steps. Activation energy was estimated to be around 42.2 kJ/mol. Reaction rate, order of reaction and its kinetics were studied and their correlations were verified with experimental data.

CHAPTER 1

INTRODUCTION

1.1 Nanoscience and Nanotechnology

In recent years, the advancement of science and technology has led to the development of *micro* and *nano*-scale materials that enable our modern life to be much simpler, more comfortable and more convenient. The ability to see nano-sized materials has opened up a world of possibilities in a variety of industries and scientific endeavours. A nanometre (nm) is one-billionth of a meter, smaller than the wavelength of visible light and a hundred-thousandth the width of a human hair. The concept of nanotechnology was first proposed by the Nobel laureate Richard P. Feynman in 1959 and later the term “*nanotechnology*” was coined by Norio Taniguchi in 1974 (Fortina *et al.*, 2007)

Nanotechnology is defined as the study and use of structures between 1 nm and 100 nm in size. It is essentially a set of techniques that allow manipulation of properties at a very small scale. Figure 1.1 represents the range of materials from millimetre to nanometre scale.

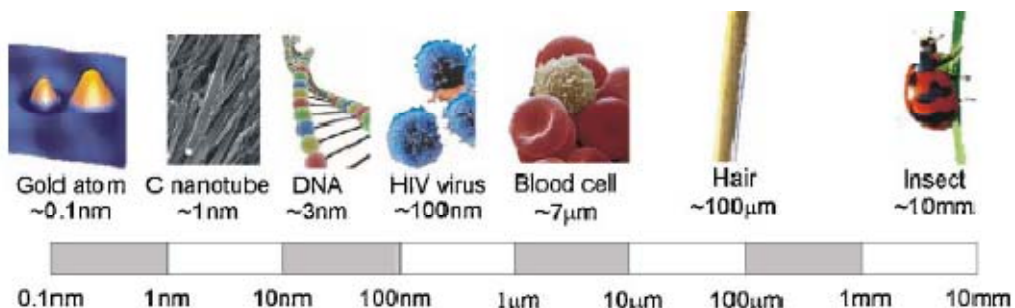


Figure 1.1. Scale showing the range of materials from mm to nm (Serrano *et al.*, 2009).

At *nano* level, the materials are designed through process that exhibit fundamental control over the physical and chemical attributes of molecular-scale structures with one of its dimension of about 1 – 100 nm. The special applications in the current technology include ever smaller computer chips, custom-designed drugs, and materials with vastly increased strength based on arrangement of their molecules (such as carbon nanotubes).

1.2 Future scope of Nanotechnology

Nowadays, nanotechnology has spread its roots in almost all areas ranging from energy storage equipment to stain resistant fabrics. Diversified fields of application in nanotechnology on various sectors are shown in Figure 1.2.

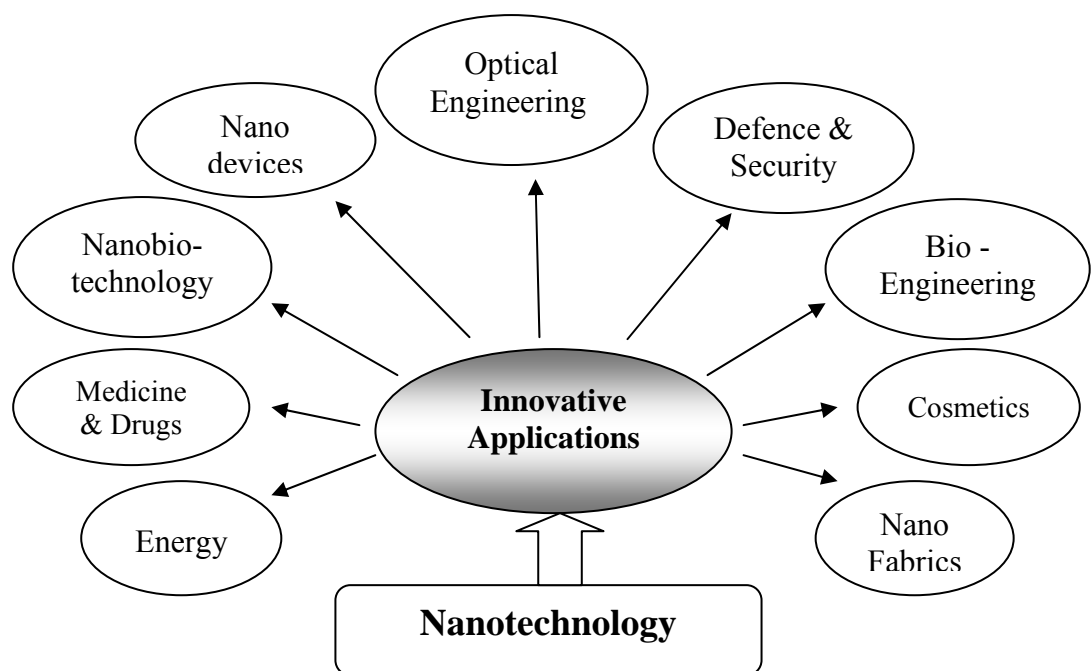


Figure 1.2. Diverse applications of nanotechnology in today's life (Bioinfobank, 2010).

Nanotechnology has the prospects to revolutionise healthcare for the next generation. There are three key areas in which it could do this: diagnosis, prevention and treatment. It offers new solutions through particles and filter systems that can bind and remove or de-activate pollutants within land, sea and air. The promise is of more efficient use of resources, renewable energy, environmental monitoring and many more benefits. It has driven the development of super capacitors through the production of novel nanomaterials with increased surface area. Such materials can accommodate much more charge than conventional materials, thus increasing energy density and power output many fold.

At present, nanotechnology has reached the electronics industry with features in microprocessors now less than 100 nanometres (nm) in size (Intel's Prescott processor uses 90 nm size features) (thekra-nanotechnology, 2010). It offer a new approach for the electronics industry in the form of new circuit materials, processors, information storage and even ways of transferring information such as optoelectronics. Nanotechnology is present in a number of consumer goods, and the number has been drastically increasing in recent years. Figure 1.3 shows the global prospects of nanotechnology in various industries and its estimated growth towards a trillion dollars in the forth-coming years.

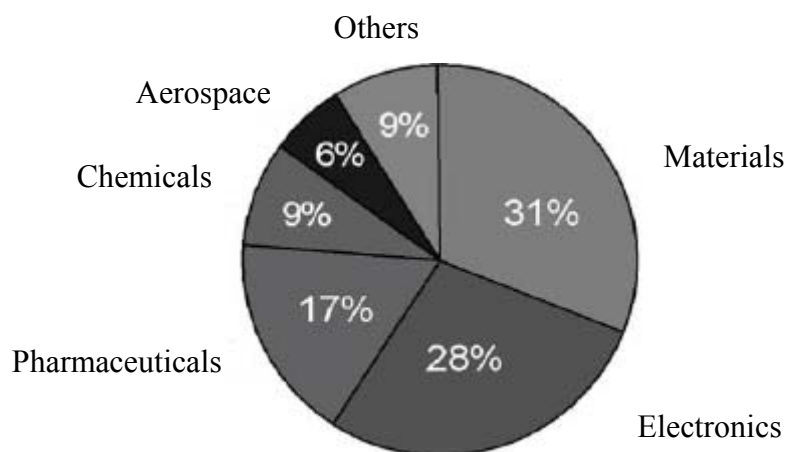


Figure 1.3. Nanotechnology related area of services and future estimation by National Science Foundation (NSF), USA (Interdisciplines, 2010).

1.3 Carbon and its classification

Carbon plays exceedingly predominant role in our daily life. It is present in many things that we use in our routine life. Carbon atom is distinct amongst all the elements that are found in nature. This uniqueness facilitates carbon to form millions of organic compounds. The electronic structure of carbon in the ground state is $1s^2 2s^2 2p^2$. Carbon forms bonds with its neighbour atoms due to the re-arrangement of the electrons in the orbitals via hybridization process. Based on sp^3 , sp^2 and sp hybridization types, the nature of carbon bond formation differs and hence responsible for the formation of different orientation, such as tetrahedral, planar and chain structures. Different carbon structures formed are called allotropes. Carbon exists in three pure crystalline forms: diamond (3-D form), graphite (2-D form) and fullerenes (0-D form). All other forms are amorphous allotropes of carbon. Each exhibits markedly different properties due to the different structures they adopt. The most recently identified allotrope of carbon is carbon nanotubes (CNTs). They

consist of carbon atoms bonded into a tubular shape. Classification of carbon based on its nature of occurrence is shown in Figure. 1.4.

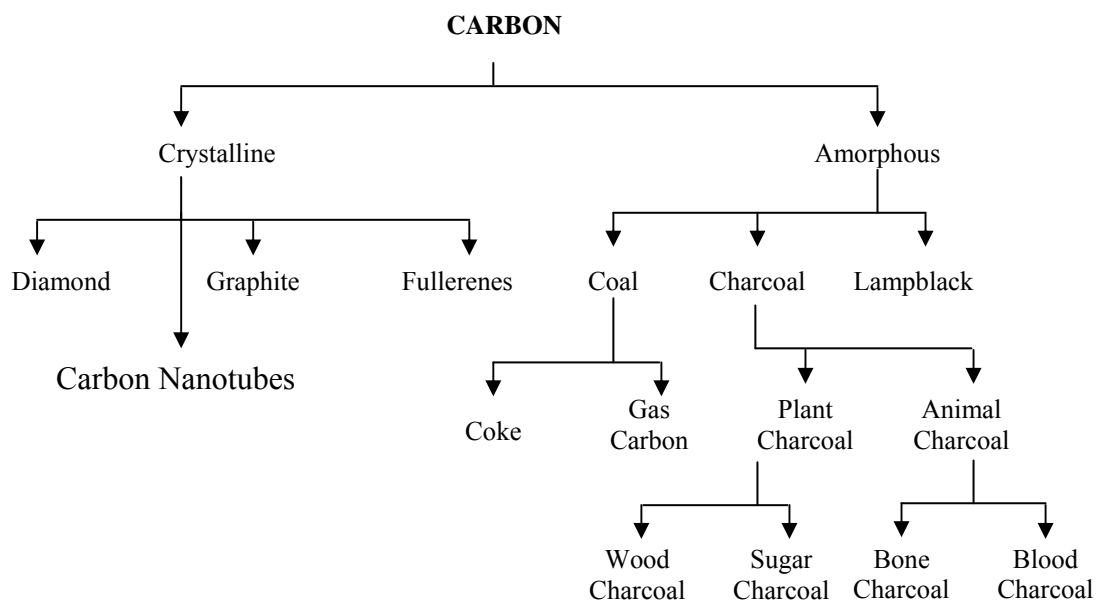


Figure 1.4. Classification of carbon based on its nature (Baddour and Briens, 2005).

Graphite is a form of carbon, in which each atom is bonded trigonally to three others in a plane composed of merged hexagonal rings, similar to those in aromatic hydrocarbons. The network is 2-dimensional, and the flat sheets are loosely bonded through weak van der Waals forces. In diamond, each atom is bonded tetrahedrally to four others, thus making a 3-dimensional network of puckered six-membered rings of atoms. The buckyballs are large molecules formed solely of carbon bonded trigonally, forming spheroids (like soccer ball-shaped structure C_{60} buckminsterfullerene). CNTs are structurally similar to buckyballs, but each atom is bonded trigonally in a curved sheet that forms a hollow cylinder. The different allotropes of carbon are shown in Figure 1.5.

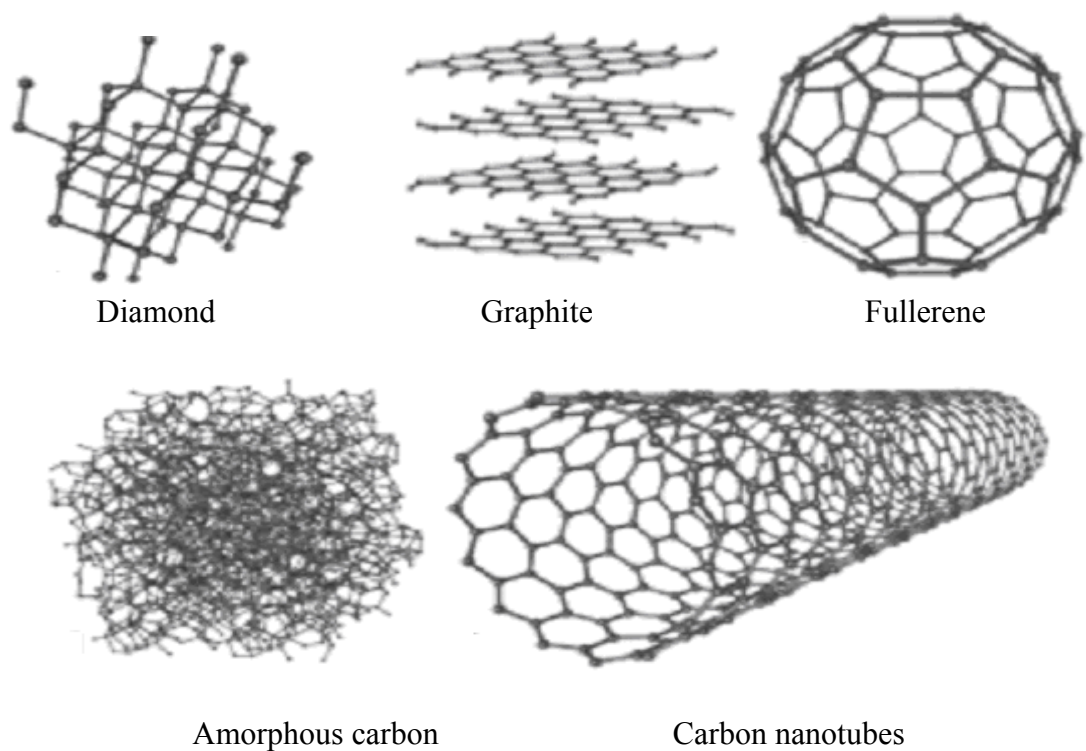


Figure 1.5. Allotropes of carbon and their structural arrangement (Nanoage, 2010).

1.4 Carbon nanotubes (CNTs) morphologies and its properties

Carbon Nanotubes (CNTs) are a new form of pure carbon that is perfectly straight tubules with diameter in nanometres, length in microns and properties close to those of an ideal graphite fibre (Ajayan *et al.*, 2000). An ideal nanotube can be considered as hexagonal network of carbon atoms that has been rolled up to make a seamless hollow cylinder. These CNTs possess unique nano structures with remarkable mechanical and electronic properties that find the use of these materials in various applications. The history of carbon Nanotubes began with the development of fullerenes by Kratschmer *et al.* (1990). After that in 1991, Sumio Iijima of Japan was the first to report about CNTs having multi-walled structure (MWNTs) synthesized by arc-discharge evaporation technique (Iijima, 1991).

MWNTs consist of multiple rolled layers (concentric tubes) of graphite having an inner layer distance approximately 3.4 Å. Further in 1993, Donald S. Bethune (IBM) and Sumio Iijima (NEC) independently discovered single-wall carbon nanotubes (SWNTs) using similar arc discharge method. In this method, a graphite anode containing a metal catalyst (Fe or Co) was used to obtain SWNT from the soot in the gas phase, but not from the cathode deposit (Journet *et al.*, 1997). Various morphologies of CNTs based on their wall structure were categorised as shown in Figure 1.6.

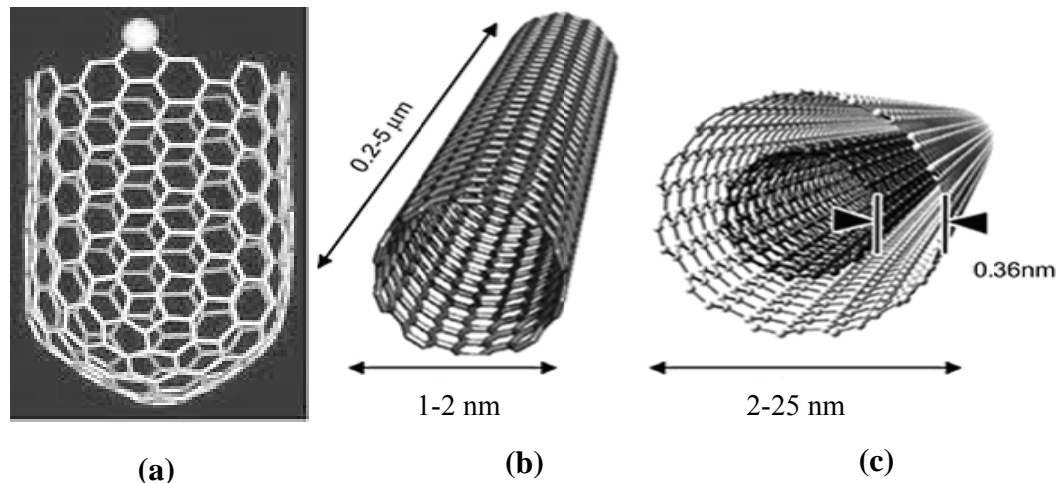


Figure 1.6. Structures of (a) Unique CNT, (b) Single-walled and (c) Multi-walled carbon nanotubes (Danmengshuai, 2010).

Most SWNTs have a diameter of ~ 1 nm, with a tube length that can be many millions of times longer. The structure of SWNTs can be formed by wrapping a one-atom-thick layer of graphite called graphene into a seamless cylinder. The way the graphene sheet is folded is represented by a pair of indices (n,m) called the chiral vector (as shown in Figure 1.7). The integers n and m denote the number of unit vectors along two directions in the honeycomb crystal lattice of graphene. If $m = 0$, the nanotubes are called "zigzag". If $n = m$, the nanotubes are called "armchair".

Otherwise, they are called "chiral". The important properties of nanotubes are functions of tube chirality. The significance of tube chirality (n,m) is its direct relation with the electronic, optical, magnetic and other properties of the nanotube.

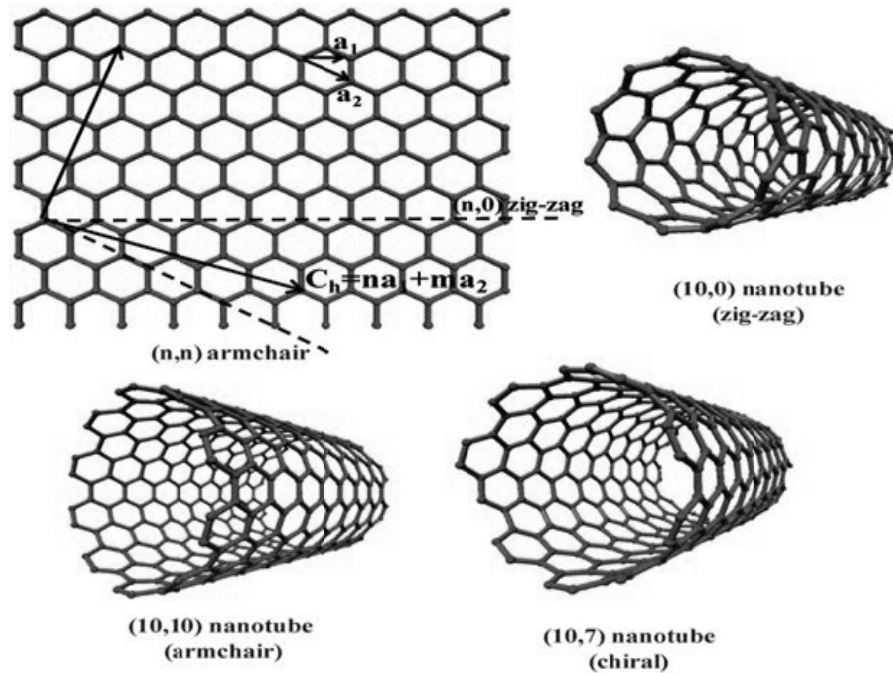


Figure 1.7. Chirality and related structure of CNTs (Wildoer *et al.*, 1998).

There are 3 main methods for the production of CNTs. They are 1) electric arc-discharge 2) laser vaporization and 3) chemical vapour deposition (CVD) method. Other techniques include electrolytic synthesis and solar production method (Agboola *et al.*, 2007). Generally, CNTs synthesized by the high-temperature electric arc or laser vaporization processes have less structural defects, in addition to superior mechanical and electrical properties, than the low-temperature chemical vapour deposition processes. Electric arc and laser ablation processes are limited due to their elaborate configurations. However, catalytic chemical vapour deposition operates at lower temperature and is technically simpler than arc and laser ablation methods. It is

considered to be the economical route for higher production of CNTs. Further, the description of each synthesis methods will be discussed in the Literature Review section.

The various properties of CNTs result directly from their structural affiliation to graphite. A SWNT can be metallic and semiconducting, dependent on its tube chirality. Meanwhile, MWNT can be either metallic or a semi-conducting. This is due to their dominating larger outermost tube (Meyyappan, 2004). Both SWNTs and MWNTs are interesting nanoscale materials from applications perspective because CNTs (a) have very good elastic-mechanical properties for use as light – weight reinforcing fibres for functional composite materials; (b) can be both metallic or semiconductor leading to the possibility of use in field – effect transistors and sensors and nanotubes hetero-junctions in electronic switches; (c) are high aspect ratio objects with good electronic and mechanical characteristics leading to their use in field emission displays and various types of scanning probe microscope tips for metrological purposes and (d) are also hollow, tubular molecules with large surface area suitable for packing material for gas and hydrocarbon fuel storage devices, gas or liquid filtration devices, and molecular–scale controlled drug–delivery devices.

The high tensile strength of CNTs is closely related to that of graphene. The graphitic sp^2 bond in CNTs is 33% stronger than the sp^3 bond of diamond (Dervishi, 2009). In contrast to planar graphenes, the cylindrical shape provides the CNTs with structural stability. The Young's modulus of CNTs bundles exceeds 1TPa, which is predominantly beneficial for the high strength properties of composites based on nanotubes. The main challenges during synthesis are to achieve a uniform dispersion

and alignment of nanotubes in a matrix and matrix to CNTs load transfer. Current emphasis is on advancing both the science and applications stemming from these mechanical properties. As defects strongly influence the mechanical properties of nanotubes, till date researchers are continuously working to face the challenges of controlling the synthesis process.

Table 1.1. Properties of Carbon nanotubes (Dong *et al.*, 2007)

Property of CNTs	Characteristics	Data
Geometrical	Layers	Single / Multiple
	Aspect ratio	10-1000
	Diameter	~ 0.4nm to <3nm (SWNTs) ~1.4 to <100 nm (MWNTs)
	Length	Several μm (Rope upto cm)
Mechanical	Young's Modulus	~ 1 TPa (Steel : 0.2 TPa)
	Tensile Strength	45 GPa (Steel : 2GPa)
	Density	1.33 ~ 1.4 g/cm^3 (Al: 2.7 g/cm^3)
Electronic	Conductivity	Metallic / Semi- conductivity
	Current Carrying Capacity	~ 1 TA / cm^3 (Cu: 1 GA/ cm^3)
	Field Emission	Activate Phosphorous at 1~3V
Thermal	Heat Transmission	> 3 kW/mK (Diamond : 2 kW/mK)

There has been large number of research done on electrical properties of CNTs (Dunlap, 1992; Langer *et al.*, 1996; Postma, 2001) since there is an interest in the use of CNTs in nanoscale electronic devices. The electronic properties of CNTs are dependent on the tube structures and can be used as junction between metal-semiconductor, semiconductor-semiconductor and metal-metal (Popov, 2004). There

are three types of junction: On-tube, Y- and crossed junctions. An On-tube junction can be attained by joining 2 tubes of different chiralities (Dunlap, 1992) or by chemical doping CNTs sediments (Zhou *et al.*, 2000). Y and crossed junctions are formed from Y- branched CNTs (Papadopoulos *et al.*, 2000) and crossed CNTs (Fuhrer *et al.*, 2000). These various CNTs junctions can be used to manufacture parts of nano-scale devices.

The thermal conductivity of CNTs along their axis appears superior to that of all materials including diamond, due to the benefits derived from the strength and toughness of the sp^2 bond. The CNTs also possess 1-D character that strongly limits their allowed scattering processes. CNTs remain stable up to very high temperature of 4000 K, due to their structural similarity with that of graphite. CNTs maximise their configurational and vibrational entropy similar to other low dimensional structures / polymers giving rise to thermal contraction in length and volume up to temperatures of several hundred degree celcius.

1.5 Applications of CNTs

Recent discoveries of various forms of CNTs have stimulated research on their applications in diverse fields. They are promising for the progress of innovative technological applications such as batteries, tips for scanning probe microscopy, electro chemical actuators and sensors (Baughman *et al.*, 1999; Kong *et al.*, 2001). Other recent and their broad areas of application are shown in Table 1.2.

Table1.2. Different fields of applications of carbon nanotubes.

Field of CNTs applications	References	Remarks
High tensile strengthfibres	Sandler <i>et al.</i> (2003)	SWNTs embedded into a polymer. Fibres produced with polyvinyl alcohol required 600 J/g to break, in comparison, that of bullet-resistant fibre Kevlar is 27–33 J/g
Concrete	Zhu <i>et al.</i> (2004)	CNTs increase the tensile strength, and halt crack propagation in building materials. They are able to replace steel in suspension bridges
Clothes	De Schrijver <i>et al.</i> (2009)	CNTs are used in textile industries to manufacture water proof tear-resistant clothing. Massachusetts Institute of Technology (MIT) is working on combat jackets that use carbon nanotubes as ultra-strong fibres and to monitor the condition of the wearer
Ultra capacitors	Gao <i>et al.</i> (2009)	MIT is researching the use of nanotubes bound to the charge plates of capacitors in order to dramatically increase the surface area and therefore energy storage ability
Sports equipment	Schmid (2009)	Stronger and lighter tennis rackets, bike parts, golf balls, golf clubs, golf shaft and baseball bats were recently developed
Polyethylene	Gupta <i>et al.</i> (2010)	The addition of CNTs to polyethylene increases the polymer's elastic modulus by 30%
Fire protection	Zaikov <i>et al.</i> (2010)	CNTs are used as covering material with a thin layer of buckypaper, which significantly improve fire resistance due to the efficient reflection of heat by the dense, compact layer of nanotubes or carbon fibres
Solar cells	Li & Xu (2010)	GE's CNTs diode has a photovoltaic effect. Nanotubes can replace solar cells to act as a transparent conductive film in solar cells to allow light to pass to the active layers and generate photocurrent

Table 1.2. Continued.

Field of CNTs applications	References	Remarks
Superconductor	Chae <i>et al.</i> (2010)	CNTs have been shown to be superconducting at low temperatures
Displays	Yuan <i>et al.</i> (2010)	Low-energy low-weight displays. This type of display would consist of a group of many tiny CRTs, each providing the electrons to hit the phosphor of one pixel, instead of having one giant CRT in which electrons are aimed using electric and magnetic fields. These displays are known as field emission displays (FEDs)
Hydrogen storage	Martin <i>et al.</i> (2010)	Research is currently being undertaken into the potential use of CNTs for hydrogen storage. They have the potential to store between 4.2 and 65% hydrogen by weight. This is an important area of research, since if they can be mass produced economically there is potential to contain the same quantity of energy as a 50L gasoline tank in 13.2L of nanotubes
Water filter	Upadhyayula <i>et al.</i> (2009)	Recently, CNTs membranes have been developed for use in filtration. This technique can purportedly reduce desalination costs by 75%. The tubes are so thin so that small particles (like water molecules) can pass through them, while larger particles (such as the chloride ions in salt) are blocked
Air pollution filter	Guan and Yao, (2010)	Future applications of CNTs membranes include filtering carbon dioxide from power plant emissions

1.6 Problem statement

Owing to its extra- ordinary physical and chemical properties, CNTs are one of the most fascinating materials. Among various nanomaterials, CNTs finds wide

scope and applications in many areas of science and technology. Hence, there is a huge demand for CNTs at present and in future. Nowadays, synthesis of CNTs is one of the prominent focuses of many researchers around the globe. Among the three methods of CNTs synthesis, arc discharge and laser ablation were reported to be very expensive, tedious operation involve high temperature. Though various latest strategies have been adopted in recent years to produce these expensive nanomaterials, only catalytic CVD method has found its way towards the large scale production in a simplest manner (Baddour and Briens, 2005).

During the CVD method of CNTs synthesis, usually hydrocarbon vapours will be decomposed at high temperatures (600-900 °C) by the metal catalyst over chemically inert support materials. Transition metals such as Ni, Co and Fe are the most commonly used catalysts over high temperature resistance supports with high surface area such as silica, alumina, zeolites and magnesia. Other metals such as copper, molybdenum, boron, etc, are also been used either as promoters or used in binary metal compositions to enhance the yield of CNTs during synthesis. In addition to the nature of metal catalysts and supports, several other CVD process parameters such as flow rate of hydrocarbon gas, catalyst pre-treatment condition like catalyst calcination temperature, reduction under H₂ atmosphere, reaction temperature and time play a vital role in determining the growth and yield of CNTs.

Innumerable research work has been carried out using the traditional supports and catalysts to synthesize CNTs by CVD method. It is found that growth mechanism of CNTs depends on the metal-support interactions. Stronger interactions would cause CNTs to grow with base-growth mechanism while, weaker interaction

results in tip-growth CNTs. Hence, the nature of metal catalysts and the support on which they are impregnated are found to play a major role in determining the CNTs growth mechanism along with all other CVD process parameters.

Despite several in-depth studies made on the CNTs synthesis with transitional metal catalysts and traditional supports, there are still several setbacks like high raw materials cost (especially for chemical supports like alumina, silica, zeolite and magnesia), difficulty in the removal of support from the synthesized CNTs product and expensive post-processing treatments to be made after the CVD reaction. Due to aforementioned drawbacks, CNTs ultimately have higher production cost and market price. In order to overcome the current high production cost, an initiative towards the use of low-cost and abundantly available resources like carbon materials were identified in this research project, to be used as supports for catalysts in CVD process. Some of the advantages of carbon support are, chemically inert, economically available from natural resources like wood waste, coal, etc., which possessing high surface area similar to that of traditional supports. Carbon has also been used as catalyst support in many industrial processes.

Carbon materials are also found to play a crucial role in hydrocarbon decomposition based on its nature, source of origin and surface properties. Malaysia is the world leading nation in palm oil industry and is also one of the main resources for availability of activated carbon (one of the major by-product that is available in plenty from palm industries). Thus this study explores the possibility of utilizing carbon as support for metal catalyst in catalytic CVD process towards achieving CNTs production at lower cost. In this research, the main scope is set to develop

catalysts based on carbon support and to do further experimental studies on methane decomposition to get different morphologies of CNTs. Different kinds of analysis using equipment like SEM, TEM, XRD, TPR, and online-GC are employed to characterize the developed catalyst as well as the product CNTs produced from the methane decomposition process.

1.7 Research objectives

The present study has the following objectives:

- 1) To synthesize carbon nanotubes (CNTs) over carbon supports using different transition metal catalysts (Fe, Co and Ni) via methane catalytic chemical vapour decomposition process.
- 2) To examine the effect of catalyst metal loading on carbon supports and its pre-treatment conditions like calcinations and reduction temperatures over methane decomposition reactions.
- 3) To investigate the influence of process parameters like the methane to inert ($\text{CH}_4:\text{N}_2$) gas ratio, reaction temperature and reaction time on the formation of various morphological structures of CNTs.
- 4) To compare the performance of individual catalyst in methane conversion, CNTs characteristics upon different metals methane decomposition process.
- 5) To study CNTs growth mechanism and reaction rate kinetics in methane CVD process based on the developed catalysts which result with higher catalytic activity and better CNTs.

1.8 Scope of the study

The current study deals with the development of carbon based catalyst, kinetic study of methane decomposition and reaction parameters for CNTs formation. The method of CNTs synthesis is carried out using catalytic chemical vapour decomposition of methane. During this process, the prepared catalysts are subjected to a high temperature reaction in a tubular horizontal fixed bed reactor. The reactor exit gases are analyzed using an online gas chromatography. Synthesized catalysts and product samples are characterized using surface area analyzer, scanning electron microscopy (SEM), transmission electron microscopy (TEM), thermogravimetric analyzer (TGA), temperature-programmed reduction (TPR) apparatus, X-ray diffractometer (XRD) and Raman spectroscopy.

The main objective of this study is to develop low-cost carbon based catalyst for CNTs synthesis. This approach towards the usage of carbon as support for the active metals in carbon nanotubes synthesis is to overcome the existing drawback of its high production cost. It also allows the anchoring of metal particles on a substrate which does not exhibit solid acid-base properties. In this study, transition metals like Ni, Co and Fe are considered for catalyst development, as they are already been proven and well established catalysts along with traditional support materials like silica, alumina, zeolite and magnesia. Naturally, carbon materials have surface properties that are suitable for a support which is considered to be one of the important parameters for accommodating the metal particles and its distribution over the surface, which in turn leads to different morphologies of CNTs. All of these important criteria enable us to further study about its role with respect to the interaction with active metals like Fe, Co and Ni in methane decomposition.

During catalyst development, some of the important aspects that determine the particle size distribution and metal-support interactions are metal catalyst loading, calcination and reduction temperatures. Hence, the aforementioned parameters are varied at different conditions in order to study the methane decomposition reaction. The catalyst activity and its stability during the methane CVD process are identified from methane gas conversion using chromatographic technique. After the study of individual metal catalysts and its pre-treatment conditions towards effective methane decomposition, ultimate aim of CNTs production is focussed by studying the reaction parametric conditions like reaction temperature, time, gas ratio ($\text{CH}_4:\text{N}_2$). The resultant products were analysed to study the morphologies and structure of CNTs formed over different metal catalysts. The structure and the growth mechanism of CNTs are characterized using high resolution TEM and SEM. The embedded metal particles in the nanotubes are detected by EDX. The nature of metal oxides and its reduced forms are studied using powdered XRD technique. The amorphous and graphitized carbon formed over the product samples are studied through Raman spectral analysis.

Thermal stability of the catalyst and CNTs are examined with the help of TGA. The conditions such as metal loading, calcination temperature, catalyst reduction, reaction temperature, reaction time and gas ratio, are optimized based upon parameters such as catalytic activity and its stability, higher methane conversion during CCVD and better CNTs formation over the developed catalyst. Further kinetic studies and possible reaction rate mechanism for the methane decomposition over the developed catalyst are also investigated.

1.9 Organization of the thesis

This thesis consists of six chapters. Chapter 1 (Introduction) provides a brief description about nanoscience and nanotechnology, its importance and applications in various sectors. It also discusses about different types of carbon nanotubes and its wide applications in diversified areas of science and technology. This chapter also includes the problem statement that provides some basis and rationale for the research directions while objectives followed by the organization of the thesis.

Chapter 2 (Literature Review) summarizes the earlier research works that has been carried out in the fields related to CNTs synthesis. It also includes the prominent CNTs synthesis techniques highlighting its advantages and disadvantages. Further, a review on various CVD reaction parameters and CNTs growth influencing factors is made in this chapter. Possible growth mechanism of CNTs on supported catalysts is also reviewed and thoroughly discussed. This serves as the background information about the specific problems that are addressed in this research work.

Chapter 3 (Materials and Methods) presents the details of the materials and chemicals used and the research methodology conducted in the present study. Detailed experimental setup is elaborated and shown in this chapter. This is followed by the discussion on the detailed experimental procedures, covering catalyst preparations, CNTs synthesis procedures and CVD process parameters study. Finally, the analytical techniques and the conditions set for the equipment used for various characterizations of both CNTs and catalysts are presented.

Chapter 4 (Results and Discussion) presents and discusses all important findings obtained in this study. This chapter is the main part of the thesis and it comprises of seven main sections based on the present experimental work done. The main topics in this chapter include studies on methane CVD process, the use of activated carbon as support for nickel, cobalt and iron catalysts, effects of catalyst pre-treatment, process analysis, growth mechanism and kinetic study.

Chapter 5 (Conclusions and Recommendations) reported the conclusions that are obtained from each individual study carried out in the present research and also suggests the ways to improve the present studies and make recommendations for possible future studies in this field. These recommendations and suggestions are given after taking into consideration the significant findings, the conclusions obtained as well as the limitations and difficulties encountered in the present work.

CHAPTER 2

LITERATURE REVIEW

2.1 CNTs synthesis methods

After the initial discovery of carbon nanotubes (CNTs) by Sumio Iijima in 1991, researchers around the world started their keen interest towards the synthesis techniques to develop different morphologies of CNTs, because of their fascinating properties and applications in various fields. In continuation, several methods had been adopted in the following years to prepare CNTs. The prominent techniques are as follows: (1) Arc discharge (2) Laser ablation and (3) Chemical vapour deposition. The descriptions of each method were explained in detail in the following sections.

2.1.1 Arc- discharge method

Arc-discharge is the primitive and common method of producing CNTs. This technique involves the growth of CNTs on carbon (graphite) electrodes during the direct current (dc) arc-discharge evaporation of carbon in the presence of an inert gas such as helium or argon (Popov, 2004). Figure 2.1 illustrates the arc-discharge scheme. In this technique, anode is moved towards the cathode until they are less than 1 mm apart and a current of 100 Amp passes through the electrodes, creating plasma between them. The temperature of this plasma usually reaches 4000 K. At this temperature, the graphite on the anode is vaporized and deposited onto the cathode. The diameter of the anode is normally smaller than the diameter of the cathode and both electrodes are water-cooled. Basically, two types of synthesis can

be achieved by the arc-discharge method: with or without catalyst to produce MWNTs and SWNTs, respectively (Journet *et al.*, 1997). Iijima was the first researcher to report CNTs (diameters from 4 to 30 nm and up to 1 μm in length) without catalyst in 1991. By altering the previous method, SWNTs had been produced with an impregnation of metal catalysts like Fe, Co, Ni or other bimetallic catalysts on the cathode or anode (Bethune *et al.*, 1993; Iijima and Ichihashi, 1993). Mass production of SWNTs by arc discharge was performed by Journet and co-workers using a bi-metallic Ni-Y catalyst in helium ambient gas (Journet *et al.*, 1997). This method was further modified using two graphite electrodes inclined at an angle 30° instead of conventional 180° alignment. This was known as Arc-plasma-Jet method and yielded SWNTs at a rate of $\sim 1\text{ gm / min}$ (Ando *et al.*, 2000).

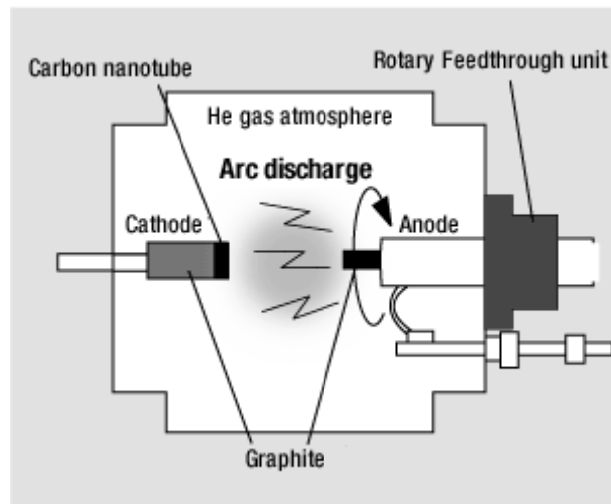


Figure 2.1. Schematic diagram of the Arc-discharge method of CNTs synthesis (Ando *et al.*, 2004).

2.1.2 Laser ablation method

The first to produce CNTs by laser ablation method was Guo *et al.* in 1995. SWNTs were synthesized by laser vaporization of a mixture of graphite and transition metals located on a target. The schematic set up of laser ablation is shown in the Figure 2.2. A pulsed (Chen *et al.*, 2005; Švrček, 2008; Stramel *et al.*, 2010) or a continuous (Bolshakov *et al.*, 2002) laser at 1200 °C was used to vaporize a target consisting of a mixture of graphite and metal catalysts, such as Co or Ni, in the presence of 500 Torr (67 kPa) helium or argon gas. Further, a modified mechanism was proposed by Scott *et al.* in 2001, in which the target was vaporized and catalyst vapours were formed rapidly. During laser ablation, a flow of inert gas (argon or nitrogen) sweeps the grown CNTs from the growth furnace to a water cooled copper collector placed just outside the furnace. The growth of these molecules continues to form SWNTs until either the catalyst clusters are too large or until the conditions have cooled. The limitation of this method is that no CNTs can be synthesized without the catalyst.

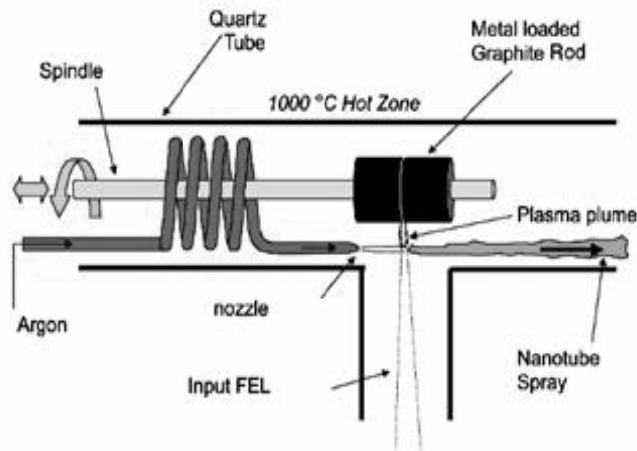


Figure 2.2. Schematic diagram of the Laser ablation method of CNTs synthesis (van der Wal *et al.*, 2003).

2.1.3 Chemical vapour deposition (CVD) method

Chemical vapours decomposition (CVD) technique was introduced by Yacaman *et al.* (1993). This was found to be an advanced, economical and low temperature method as compared to arc discharge and laser ablation methods. This process involves the decomposition of a hydrocarbon in the presence of a metal catalyst. Hydrocarbons usually used are ethylene or acetylene, which are decomposed in a tube reactor at temperatures ranging from 550 to 750°C (Popov, 2004). Figure 2.3 illustrates a CVD system. During the synthesis, the hydrocarbon enters the reactor with an inert gas at high temperature. As the decomposition of hydrocarbon occurs, carbon settles onto the catalyst, which was supported by a material such as alumina, silica, zeolites, etc. The most commonly used active metals for CNTs synthesis are iron, nickel or cobalt. Since carbon has a low solubility in these metals at high temperatures, the carbon tends to precipitate to form nanotubes (Dresselhaus & Endo, 2001).

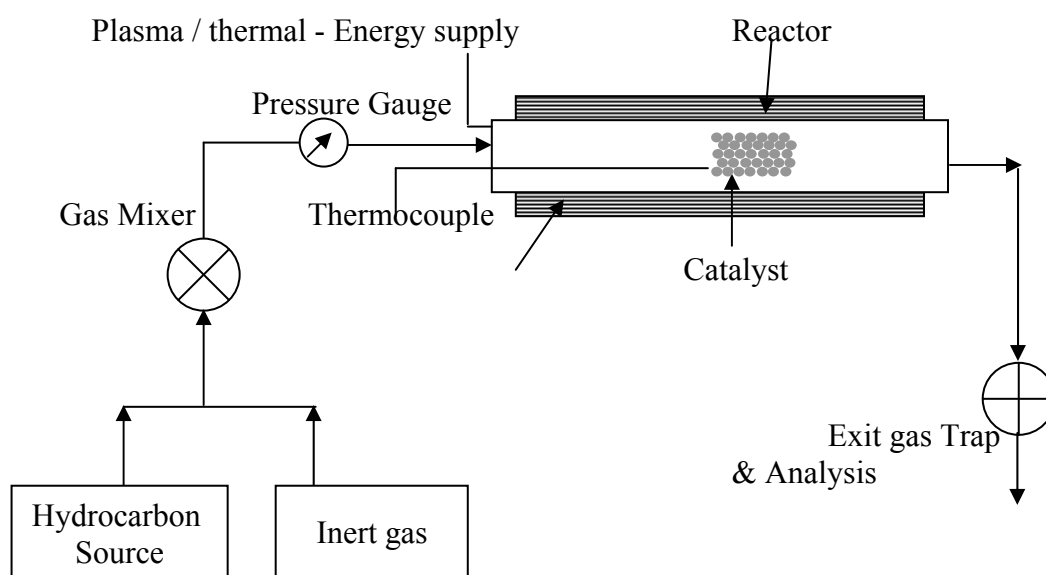


Figure 2.3. Schematic diagram of a CVD process for CNTs synthesis (Oncel and Yurum, 2006).

2.1.4 Summary

All of the above methods of CNTs synthesis have some advantages and limitations. For example, the main disadvantages of arc discharge and laser ablation methods are they require high power to generate carbon vapours from graphite rod and the requirements of sophisticated and costlier equipment. But in recent times, the focusing issue is about the selection of best and economical method for commercial production of CNTs (Serp *et al.*, 2003). Since bulk production of CNTs is becoming the most important factor, industries today are opting for the CVD technique. It is a promising technique that can be easily up-scaled to industrial production level. This technique has been reported to be the simplest method with high yield and well controlled growth process of nanotubes in larger scale. Table 2.1 highlights the summary of different CNTs synthesis methods.